# Ion-Channel Biosensors—Part I: Construction, Operation, and Clinical Studies

Vikram Krishnamurthy, *Fellow, IEEE*, Sahar Moradi Monfared, and Bruce Cornell

***Abstract*—This paper deals with the construction and operation of a novel biosensor that exploits the molecular switching mechanisms of biological ion channels. The biosensor comprises gramicidin A channels embedded in a synthetic tethered lipid bilayer. It provides a highly sensitive and rapid detection method for a wide variety of analytes. In this paper, we outline the fabrication and principle of operation of the ion-channel switch (ICS) biosensor. The results of a clinical study, in which the ion-channel biosensor is used to detect influenza A in untreated clinical samples, is presented to demonstrate the utility of the technology. Fabrication of biochip arrays using silicon chips decorated with "ink jet" printing is discussed. We also describe how such biochip arrays can be used for multianalyte sensing. Finally, reproducibility/stability issues of the biosensor are addressed.**

***Index Terms*—.**

## GLOSSARY

| | |
|---|---|
| BLM | Bilayer lipid membrane. |
| ELISA | Enzyme-linked immunosorbent assay (a biochemical technique used mainly in immunology to detect the presence of an antibody or an antigen in a sample). |
| Fab | Fragment antigen binding portion of antibody. |
| hCG | Human chorionic gonadotropin (glycoprotein hormone is produced during pregnancy and can be used for early detection). |
| $\beta$hCG | $\beta$ subunit of hCG gonadotropin. |
| gA | Gramicidin A ion channel. |
| gAglyB | Gramicidin with a glycine group linker to biotin. |
| gA5XB | Gramicidin with five aminocaproyl group linker. |
| ICS | Ion-channel switch. |
| IgG | Immunoglobin G, the most common human immunoglobin. |
| MSL | Membrane spanning lipid. |
| MSL4XB | Membrane spanning lipid with four aminocaproyl-linked biotin. |
| PCR | Polymerase chain reaction, which is a technique to amplify a single or few copies of a piece of DNA across several orders of magnitude. |
| X≡ | Aminocaproyl group. |
| 4X≡ | Four aminocaproyl groups. |
| 4XB≡ | Four aminocaproyl-linked biotin. |

Manuscript received May 11, 2009; revised August 20, 2009 and January 6, 2010. First published; current version published. The review of this paper was arranged by Associate Editor xxx.

V. Krishnamurthy and S. M. Monfared are with the Department of Electrical and Computer Engineering, University of British Columbia, Vancouver, BC V6T 1Z4, Canada (e-mail: vikramk@ece.ubc.ca; smonfare@ece.ubc.ca).

B. Cornell is with the Surgical Diagnostics Ltd., St Leonards, N.S.W. 2065, Australia (e-mail: brucec@surgicaldiagnostics.com).

Color versions of one or more of the figures in this paper are available online at http://ieeexplore.ieee.org.

Digital Object Identifier 10.1109/TNANO.2010.2041465

## I. INTRODUCTION

BIOLOGICAL ion channels are water-filled subnanosized pores formed by protein molecules in the membranes of all living cells [1], [2]. Ion channels play a crucial role in living organisms by selectively regulating the flow of ions into and out of a cell thereby controlling the cell's electrical and biochemical activities. This paper deals with construction and operation of a novel biosensor that exploits the molecular switching mechanisms of ion channels. Such ion-channel-based biosensors can detect target molecular species of interest across a wide range of applications. These include medical diagnostics, environmental monitoring, and general biohazard detection.

A novel biosensor that incorporates gramicidin A ion channels into a tethered synthetic cell membrane was developed by Cornell *et al.* [3]. Over the past few years, many novel functionalities have been added to successive generations of the biosensor [4]–[7]. These include the covalent linkage of Fab (see Glossary) to the gramicidin channels, the use of flow cells and the miniaturization of electrode dimension from 1 mm to 20 $\mu$m. Throughout this paper, we refer to this ion-channel biosensor as the ion-channel switch (ICS) biosensor.

The ICS biosensor provides an interesting example of engineering at the nanoscale. It is significant that the functionality of the device depends approximately on 100 lipids, and a single ion channel modulating the flow of billions of ions in a typical sensing event of approximately 5 min. Since the gramicidin channels (each with conducting pore of diameter 0.4 nm and length 2.8 nm) move randomly in the outer lipid leaflet of the membrane (1.4 nm thick), we can view the biosensor as a fully functioning nanomachine with moving parts. Indeed, each individual gramicidin channel diffuses randomly over an area of order 1 $\mu$m$^2$. Furthermore, the 4-nm-thick lipid bilayer is tethered 4 nm away from the gold surface by hydrophylic spacers thereby allowing ions to diffuse between the membrane and gold. This permits a flux in excess of $10^6$ ions per second to traverse each channel.

### A. Main Results

This paper describes the construction, operation, and usage of the ICS biosensor. The fabrication of the ICS biosensor has

several interesting properties that make it an appealing case study.

*1) Construction and Operation of the Biosensor:* The ICS biosensor incorporates a *self-assembled monolayer* providing enhanced stability (see literature review given shortly for a comparison with other schemes). The tethered bilayer permits 2-D diffusion of gramicidin channels that provides a remarkable gating mechanism. Since gramicidin has a terminal ethanolamine group that permits a range of chemistries, the biosensor may be prepared for use with a wide range of receptors to detect many different analytes. The ICS sensing mechanism does not require washing [unlike an ELISA assay (see Glossary)], provides large transduction amplification (millions of ions for every channel dimerization), and a high detection sensitivity since a single channel can diffuse and identify analyte molecules bound to many capture sites. The ICS biosensor also provides an objective electrical readout that is intrinsically digital. The digital output permits the use of sophisticated statistical signal processing algorithms to estimate the type and concentration of analyte.

In Section II, the construction of the biosensor is discussed in detail. The interface between the biochemical part of the biosensor and the electrical measurement system is provided via a gold surface to which the lipid bilayer containing the ion channels is tethered and a silver-coated return electrode that is immersed in the electrolyte above the biomimetic surface.

*2) Rapid Detection of Microorganisms:* The ICS biosensor provides a rapid detection mechanism for low-molecular-weight drugs to supramolecular. In Section III, we illustrate the use of the ICS biosensor for the rapid detection of the influenza A virus. One of the major advantages of using the ICS biosensor over the ELISA method is that many of the lengthy steps involved in the processing and incubation in an ELISA are no longer necessary.

*3) Multianalyte Detection Using Biochip Arrays:* In Section IV, we illustrate how sensor arrays of the ICS biosensor can be fabricated and used for multianalyte detection. A novel element in the design of these arrays is the use of a titanium oxide ring at the perimeter of the electrode opening, which serves as both a mechanical and electrical seal. A key issue in fabricating an array capable of multianalyte detection is the site-specific decoration of the chip with different antibodies. We describe this construction and show that biochip arrays can detect multiple analytes from a single sample addition to the sensor. Finally, in Section V, we discuss scale-up issues of the ICS biosensor including reproducibility of results and the challenges of stability/storage. These are key requirements for a commercial diagnostic technology.

The companion paper (Part II) deals with modeling the electrical and chemical kinetics of the biosensor to predict its performance. We also illustrate the use of statistical signal processing algorithms for the stochastic detection of analytes.

### B. Related Work

The literature on biosensors is vast. Neher provides an interesting overview of the interface between ion channels and microelectronics [8]. Several companies/research groups have developed biosensors based on synthetic lipid monolayers and bilayers. For example, OhmX Corporation is currently developing a reagentless biosensor system using self-assembled monolayers tethered to a gold surface for the electronic detection of biomarkers in clinical samples [9]. Stochastic signal analysis has been employed by Bayley's group at Oxford and has made substantial contributions in advancement of ion channel biosensors [10], [11]. The detection of single gramicidin channel currents in a tethered membrane is described in [9]. Here, we focus on the ICS biosensor currently being developed by Surgical Diagnostics Pty Ltd., as an important example of an ion-channel-based biosensor. We provide a review of related work in biosensors involving ion channels and tethered lipid membranes shortly.

The first attempt at developing a practical membrane-based biosensor device was reported in [12]. The poor stability of the receptor–membrane complex limited the range of applications of the device. One of the first examples of a functionally active biomimetic surface was reported in [13], in which an active cytochrome C was incorporated into a tethered membrane.

The stabilization of the *bilayer lipid membrane* (BLM) has been a central theme in the development of ion-channel biosensors [14]. Many strategies have been developed. The primary focus has been on physisorbing or chemically attaching a layer of hydrocarbon to a silicon [15], hydrogel [16], polymer [17], or metal surface [18]. Subsequently, a second layer of mobile lipids is fused onto the tethered monolayer to form a tethered BLM. Earlier works on BLM stabilization is reviewed in [19] and [20]. In [21], peptide nanotubes have been fabricated within a supported self-assembled monolayer. The ICS biosensor employs an alkane disulphide bond to stabilize the BLM at the electrode surface.

A key requirement of an ion-channel biosensor is to engineer a switching mechanism that modulates the flow of ions when an analyte is detected [7]. Mechanisms range from antichannel antibodies that disrupt ion transport [22], to molecular plugs that block the channel entrance [23]. OmpF porin channels from *Escherichia coli* were incorporated into a tethered BLM and their conduction modulated using the channel-blocker colicin [24]. All mechanisms proposed so far have had a very limited range of application and require reengineering for each new analyte. The ICS, while using ion-channel transduction provides a mechanism that may be adapted to many different classes of target.

Miniaturization and patterning are two further opportunities for tethered membrane technologies [25], [26]. The functionalities, which may be brought to tethered bilayers are becoming extensive. Topographical templates for chemoselective ligation of antigenic peptides to self-assembled monolayers have been fabricated in [27].

The remainder of this paper is organized as follows. Section II explains the details of the operation of the biosensor in detection of large and small analytes. Section III provides the details of a study performed using the ICS biosensor to detect influenza A in clinical samples. Section IV discusses fabrication issues such as multiplexing and multianalyte detection capabilities of the biochip array. Section V discusses methods for improving

stability as well as storage capability of the ICS biosensor. Our companion paper (Part II) deals with modeling, analysis, and signal processing of the ICS biosensor. It is hoped that these four aspects, namely, construction, modeling, analysis, and signal processing, provide the reader with an interesting case study that can be suitably modified to other types of biosensors.

## II. Construction and Operation of ICS Biosensor

In this section, we discuss the fabrication and operation of the ICS biosensor. This discussion forms the basis for modeling the biosensor dynamics in the companion paper (Part II).

### A. Principle of Operation

The low-molecular-weight bacterial ion-channel gramicidin has been used (see [3] and [28], see also [6] for a review), as the basis of a biosensor platform with a range of applications for the detection of low-molecular-weight drugs, large proteins, and microorganisms [29], [30]. As described earlier, the ICS biosensor employs a lipid monolayer tethered via a disulphide group to a gold surface. The membrane is separated from the gold surface by an ethylene glycol spacer that provides a reservoir for ions permeating through the membrane. The transduction mechanism depends on the properties of gramicidin A within a BLM. Gramicidin monomers diffuse within the individual monolayers of the BLM. The flow of ions through gramicidin only occurs when two nonconducting monomers align to form a conducting dimer. The gramicidin channels within the tethered inner leaflet of the lipid bilayer are also tethered to the gold electrode. Also, attached to the gold surface as part of the inner leaflet are membrane-spanning lipids. The arrival of analyte cross-links antibodies attached to the mobile outer layer channels to those attached to membrane spanning lipids. Due to the low density of tethered channels within the inner membrane leaflet, this anchors them distant, on average, from their mobile outer layer partners. Gramicidin dimerconduction is thus prevented and the biosensor admittance decreases. Applying a small alternating potential between the gold substrate and a reference electrode in the test solution generates a charge at the gold surface that causes electrons to flow in an external circuit.

The membrane stability is primarily enhanced by tethering the inner membrane leaflet to the gold surface. However, additional stability is achieved by substituting a major fraction of the tethered lipids with archaebacterial lipids. These are lipids modeled on constituents found in bacteria capable of surviving extremes of temperature and hostile chemical environments. Characteristics of these lipids are that the hydrocarbon chains span the entire membrane and that all ester linkages are replaced with ethers [31], [32]. BLM films have previously been formed from archaebacterial lipids and resulted in membranes that are stable to temperatures in excess of 90 °C [33]. A stable membrane incorporating ion channels can be self-assembled on a clean, smooth gold surface using a combination of sulphur–gold chemistry and physisorption [34]. Most studies of the ICS biosensor have used antibody Fab fragments as the receptor; however, the approach has also been demonstrated to operate using oligonucleotide probes, heavy metal chelates, and cell-surface receptors.

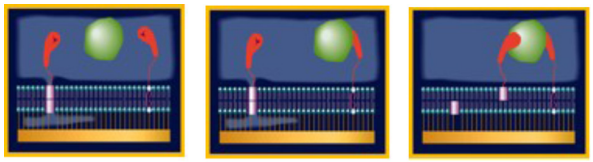


Fig. 1. Large analyte transduction mechanism. The binding of analyte (green) to the antibody fragments (Fab) (red) causes the conformation of gramicidin A to shift from conductive dimers to nonconductive monomers. This causes a loss of conduction of ions across the membrane. The scale can be visualized by the fact that the tethered lipid bilayer is 4 nm thick.

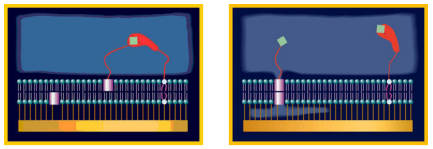


Fig. 2. Small analyte transduction mechanism. In the absence of analyte, the mobile channels cross link to antitarget Fabs anchored at the tether sites. Dimer formation is prevented and the biosensor conductance decreases. The introduction of analyte competes off the hapten (target analog) and increases the biosensor conductance.

### B. Large and Small Analyte Detection

Large analytes include proteins, hormones, polypeptides, microorganisms, oligonucleotides, DNA segments, and polymers. In the same manner that an ELISA sandwich assay may be developed based on a complementary antibody pair, the ICS biosensor may be adapted to the detection of any antigenic target for which a suitable antibody pair is available. The bacterial ion-channel gramicidin A is assembled into a tethered lipid membrane and coupled to an antibody targeting a compound of diagnostic interest. The binding of the target molecule causes the conformation of the gramicidin channels to switch from predominantly conducting dimerto predominantly nonconducting monomers, as shown in Fig. 1. For target analytes with low molecular weights such as therapeutic drugs where the target is too small to use a two site sandwich assay, a competitive adaptation of the ICS is available. This is shown in Fig. 2.

## III. Rapid Detection of Influenza A Virus in Clinical Samples

Experimental results for detection of influenza A virus using the ICS biosensor are detailed in this section. Influenza is a highly contagious respiratory infection that is spread by aerosol transmission or close personal contact. Rapid detection of the virus is crucial for prompt patient management and implementation of public health alert and control measures. The ICS biosensor offers a rapid method for the detection of microorganisms within 10 min at room temperature, without the attendant time-consuming steps of specimen extraction,

specimen washing, and incubation that are currently necessary in an ELISA or PCR test for virus detection [35], [36].

### A. ICS Biosensor for Rapid Influenza A diagnosis

A complementary pair of monoclonal antibodies were selected for reactivity to a specific strain of influenza A subtype. Fab fragments were prepared from two commercially available influenza A nucleocapsid-specific monoclonal antibodies and fragmented using papain digestion (www.piercenet.com) and biotinylated with iodoacetyl-LC-biotin according to a proprietary method that was developed in-house. An equimolar mix of the two monoclonal antibodies was used. Comparison was made with a commercial kit obtained from Medix Biochemica (www.medixbiochemica.com) and by culture. The Medix test kit consisted of a chromatographic strip paper impregnated with influenza A antibodies. An internal control was included in the test strip. After treating the specimen in the extraction solution for 5 min at room temperature, the immunochromatographic strip was immersed into the treated sample mix for an additional 10 min and read against a color standard. The culturing techniques were as previously reported [35], [37].

### B. Clinical Samples

Two groups of respiratory samples were collected across the state of South Australia and tested to assess the effects of interferences in the untreated clinical samples and the sensor response to the targeted influenza A virus.

1) Group 1: This group consisted of 74 samples drawn from nasopharyngeal aspirates, sputum, bronchial or tracheal aspirates, nose, and throat swabs during the period July–August 2006. The samples were stored at 4 °C, and tested within two days by ICS, Medix as well as by culture. However, during the period July–August 2006, when Group 1 samples were collected, no cases of influenza A occurred in South Australia. Therefore, the samples in Group 1 serve as a useful test for false positives.
2) Group 2: This group consisted of 34 randomly selected samples that had been collected during an outbreak of influenza A in July–September 2005. These samples had been stored at −70 °C. (The number of clinical samples in this group was limited by the sample populations the authors were able to negotiate from the South Australian government.) These specimens had previously been submitted for routine virus culture.

### C. Results of Influenza A Trial

The test results for Group 1 and Group 2 were analyzed in terms of sensitivity, specificity, positive predictive values (PPVs), and negative predictive values (NPV). These are defined as

$$\text{Sensitivity} = \frac{\text{number of true positives}}{\text{number of true positives} + \text{number of false negatives}}$$

$$\text{Specificity} = \frac{\text{number of true negatives}}{\text{number of true negatives} + \text{number of false positives}}$$

TABLE I
COMPARISON OF ICS AND MEDIX RAPID TESTS WITH CULTURE FOR DETECTION OF INFLUENZA A VIRUS IN 34 RESPIRATORY SPECIMENS

| | ICS % | Medix % |
|---|---|---|
| Sensitivity | 52 | 57 |
| Specificity | 82 | 100 |
| Positive Predictive value | 86 | 100 |
| Negative Predictive value | 45 | 52 |

$$\text{PPV} = \frac{\text{number of true positives}}{\text{number of true positives} + \text{number of false positives}}$$

$$\text{NPV} = \frac{\text{number of true negatives}}{\text{number of true negatives} + \text{number of false negatives}}. \quad (1)$$

1) Group 1: Of 74 samples in Group 1, no influenza A virus was detected using the ICS, the Medix kit, or by culture. Thus, the ICS did not yield false positives. Also, using culture or antigen ELISA [35], [37], it was found that 14/74 of the samples yielded a positive result for influenza B, adenovirus, respiratory syncytial virus, or parainfluenza 3 virus. This means that the ICS showed no cross-reactivity with unrelated viral antigens or interference by heterogeneous respiratory specimens. These results illustrate the specificity of the ICS.
2) Group 2: The 34 samples in Group 2 were tested using the ICS and Medix test. The specimens were diluted with an equal volume of phosphate buffer saline (PBS) prior to addition to ICS and Medix test. When compared to the culture as reference, the ICS and Medix tests showed very similar sensitivities, specificities, PPVs, and NPVs in detecting influenza A virus. The results are shown in Table I.

Thus, the addition of fresh or frozen clinical samples directly to the ICS sensor permits a rapid determination of the presence of influenza A virus without the need for detergent disruption or sample preparation with very similar results to existing commercial immunochromatographic test strips. After this trial, the importance of sample flow on detection sensitivity of the ICS biosensor has been explored and it was found that a substantial improvement resulted from sample flow rates of 10–50 $\mu$L/min. Future trials will incorporate a modified test element incorporating analyte flow during data acquisition.

## IV. BIOCHIPS AND MULTIANALYTE DETECTION

### A. Biochip Arrays

Sensor arrays have been fabricated using silicon nitride, silicon carbide, and glass substrates. Using this format, a multianalyte-detection capability is demonstrated. Multianalyte detection is an advantage as it permits onboard calibration to correct for systematic variations that can occur across an electrode array and to correct for electrode-to-electrode variation between different sensors. A novel element in the design of these arrays is the use of a titanium oxide ring at the perimeter

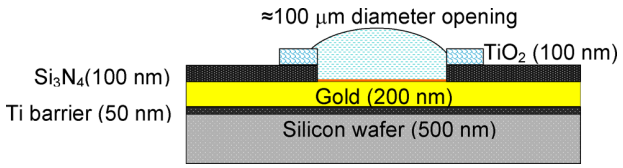


Fig. 3. Cross section of one element in a silicon chip sensor array. The design incorporates five layers: 1) an underlying silicon wafer, 2) a 50 nm titanium (Ti) barrier, 3) a 200 nm gold layer, 4) a 100 nm silicon nitride ($Si_3N_4$) layer and a patterned ring of titanium oxide ($TiO_2$). The titanium oxide ring is designed to provide a hydrophilic surface at the membrane edge.

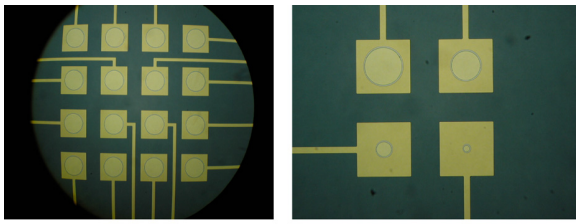


Fig. 4. (a) Optical microscopy image of a 16-element sensor array with 150 $\mu$m diameter electrodes. The apparently square geometry of the sensor elements arises from the gold being patterned as rectangles and the silicon nitride openings being round. The thin (100 nm) and transparent silicon nitride allows the gold to be viewed through the nitride layer. Also visible is the light gray 2 $\mu$m wide titanium oxide ring. (b) Optical microscopy image of a test array with four electrode elements of 150, 100, 50, and 20 $\mu$m diameter.

of the electrode opening. The titanium ring is designed to provide a mechanical seal for the outer leaflet preventing it from diffusing beyond the area of the tethered inner leaflet lipids. In addition, the titanium seal retains water during the patterning of antibodies, and during the dry down process for storage. A schematic of the design of an element in a silicon chip is shown in Fig. 3.

Examples of electrode arrays recorded by optical microscopy are shown in Fig. 4. Fig. 4(a), illustrates a 16-element array of 150 $\mu$m diameter electrodes. Fig. 4(b) depicts a test array of four electrodes ranging from 150 to 20 $\mu$m diameter. A consequence of reducing the electrode diameter from 150 to 20 $\mu$m is a reduction of the membrane capacitance and an increase in the biosensor resistance. Both measures scale with membrane area, the capacitance linearly, and the resistance inversely.

Although the impedance of these electrodes is dependent on area, the time constant of the response is independent of area. A dependence is expected, however, when the spacing of the ion channels or antibodies are comparable to the electrode dimensions. In the present case, these spacings are approximately 0.1–1 $\mu$m, far smaller than the smallest 20 $\mu$m diameter electrode reported here. However, one consequence of using an electrode array to measure the target species concentration rather than a single electrode of comparable area is the improvement in the quality of estimating the response rate. In fact, an exponential fit to the admittance decay curve measured across 16 electrodes yielded coefficients of variation (standard deviation/mean) of well below 10%. This indicates that the silicon chip fabrication procedures can provide a highly reproducible electrode geometry and structure. The distributed sensing array possesses a statistical improvement of 16 independent measurements rather than one. A further benefit of miniaturization is the detection of single channel noise that permits stochastic analysis, which is discussed in the companion paper.

### B. *Multianalyte Detection*

Sensor arrays also have the ability to measure multiple target concentrations from a single sample addition to the sensor. A key problem when fabricating an array capable of multianalyte detection is the site-specific decoration of the chip with different antibodies. The approach used here is shown in Fig. 5. A fluid-handling spotter (sciFlexarrayer leased from Scienion AG, Berlin) was loaded with the appropriate antibody solution and directed to a chip surface that had been partially dried from glycerol, trehalose, polyvinylpyrrolidone, or their combinations.

The lower size limit of the electrodes was determined by the resolution achievable by the spotter-surface characteristics and not the constraints of the electrode–membrane characteristics. The limiting dimension set by the spotter-surface combination was 80 $\mu$m diameter, whereas the limit set by the electrode–membrane combination was 10 $\mu$m. Fig. 5 shows an example of a chip array with four arbitrary antibody receptors, i.e., one quadrant, contains four electrodes, with the pregnancy hormone human chorionic gonadotrophin ($\beta$hCG), two quadrants have antibody receptors for influenza A, and a further quadrant uses the reference receptor to a target not in the test sample. Fig. 6(a) shows the response to four samples containing either 150 mIU/mL $\beta$hCG, 100 ng/L influenza A virus or neither. The reference electrode cluster yielded a null result to all three challenges; the $\beta$hCG cluster yielded a positive response (reduction in admittance read as a negative slope) to the 150 mIU/mL$\beta$hCG sample but zero to the influenza A challenge, whereas the influenza A clusters yielded a positive result to challenge with influenza A but zero to $\beta$hCG. Fig. 6(b) shows the layout of the four quadrants. These data show the ability of an electrode array to detect multiple target species in one sample addition. In this case, the sample volumes used were 100 $\mu$L but these can be reduced to 10–20 $\mu$L using a coplanar return electrode.

## V. Scale-Up Issues

Reproducibility of results is essential for calibrating a sensor. Also, stability and storage are critical issues for biosensors. We discuss these issues shortly.

### A. *Reproducibility*

Variation in the sensor performance occurs between test elements within a single chip and between chip to chip. Custom-fabricated chips were supplied by Micralyne, Edmonton, Canada. The line resolution of standard silicon foundry techniques substantially exceeds the requirements of the BioChips used here. Silicon was chosen as a platform for scaling-up sensor production since it was viewed as a mature technology that

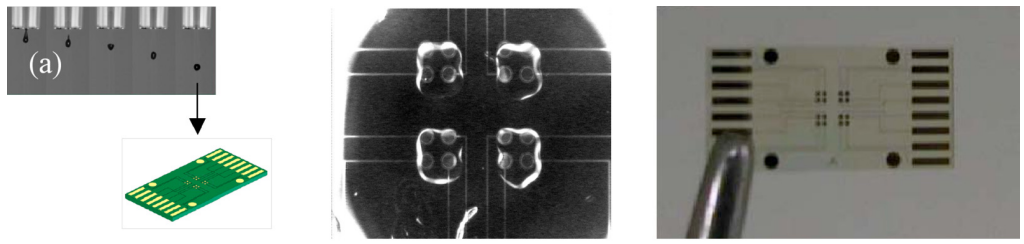


Fig. 5. (a) Site-specific coating was achieved by directing a metered volume of biotinylated antibody Fab onto an electrode element (230 $\mu$m diameter) in the array. The electrode surface was pretreated with 2%–5% trehalose solution and dried prior to spotting the surface. Prior to spotting, the membranes had been assembled to a common structure across all electrodes, including a streptavidin linker to the ion channels and membrane spanning lipids. (b) sciFlexarrayer (Scienion AG, Berlin) provided a stream of 20 pL volume drop. Typically, 15 drops were applied to each electrode resulting in 1.2 nL per quadrant of four electrodes. Each quadrant received a different biotinylated antibody fragment. (c) Chip used here was a cluster of four 2×2 electrode arrays—each 230 $\mu$m diameter on either a glass or silicon substrate.

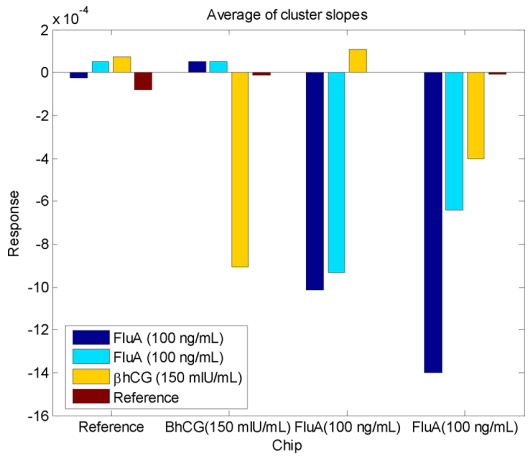


Fig. 6. (a) From left to right, the first set of bars correspond to electrode with no receptors, second set correspond to electrodes with $\beta$hGG receptors, third and fourth set contain influenza A receptors. Chip challenged with single sample possessing 150 mIU/mL $\beta$hCG and 100 ng/mL influenza A virus. (b) Array geometry and the distribution of antibodies on each of the four clusters.

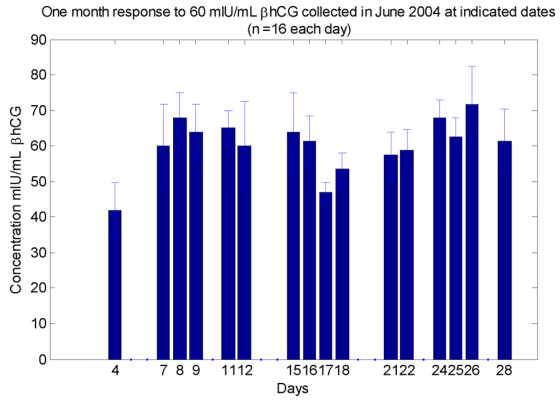


Fig. 7. Daily means of 16 estimates of 60 mIU/mL $\beta$hCG in PBS at 30 °C over a one-month period. Similar results were obtained over a 12-month period.

operated within a highly controlled, clean environment. However, an unexpected problem arose in the adaptation of standard photolithographic approaches to the fabrication of patterned surfaces for use in Au-alkanethiol-based sensors. The etch procedures employed to expose the patterned gold seriously contaminates the gold surface in a manner that we have been unable to totally reverse. Cleaning solutions such as Piranha followed by deionized water and ethanol could achieve a functioning device but the longer term stability was seriously compromised. High-energy argon ion milling of the surface was necessary immediately prior to coating the thiol or disulphide species regardless of the wet-cleaning process employed. The optimal approach is to vary the lithographic process steps to permit a deposit gold last sequence, which although requiring a final masking step, achieves the best results.

Monitoring sensor performance over many batches provides an estimate of the batch-to-batch variation in performance. Fig. 7 shows a one-month record of response to 60 mIU/mL $\beta$hCG, run without calibrators or any internal corrections for an array of 16 measures on a plastic slide. Each day represents an average of 16 measures from one array and over the month from 16 separate arrays. The sample challenge was a standard solution of 60 mIU/mL $\beta$hCG. The average daily coefficient of variation over 16 measures was 12% and the coefficient of variation of the daily means over the 16 arrays measured during the month was 4.7%. These measures were performed in PBS at 30 °C on sensors made that day.

A major step towards achieving a quantitative test is to provide an onboard calibrator to correct for daily variation. This is particularly important when measurements are made from serum or blood where matrix variations cause substantial changes to

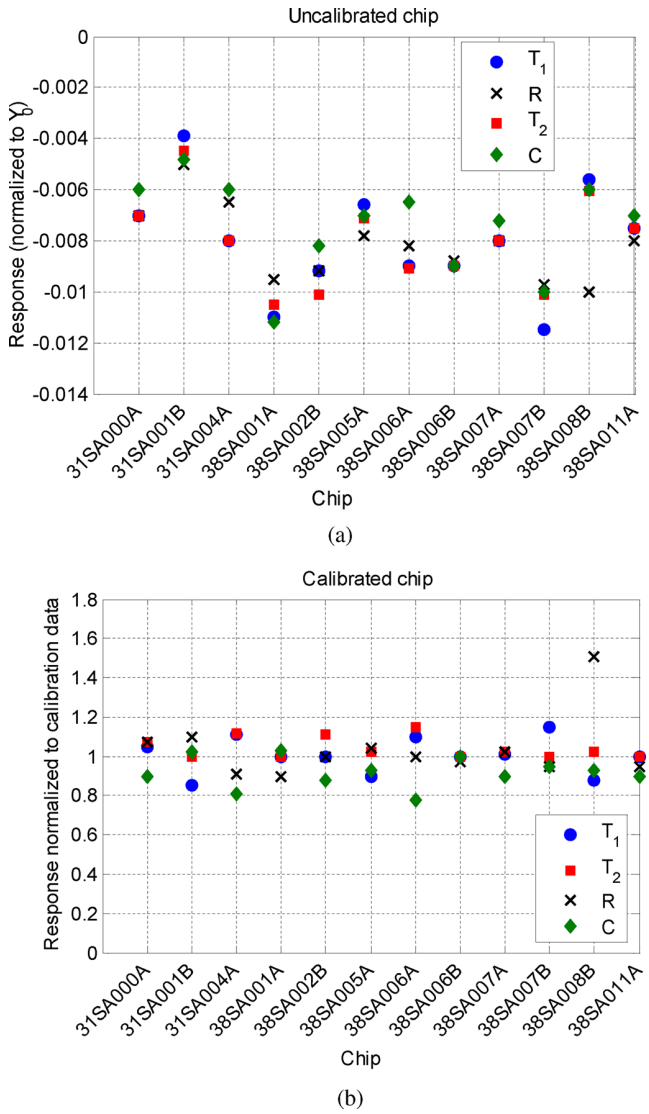


Fig. 8. Improvement in reproducibility that can be achieved by employing a calibrator (a) Uncorrected response rate to a challenge by analyte. $T_1$ and $T_2$ are two tests of the target concentration, $C$ is a calibration measure, and $R$ is a reference channel that permits a differential measure. The latter is used in blood or serum where matrix artifacts are minimized through the use of a differential reading between the test and reference electrode. The data have been normalized to the gating amplitude only. (b) Response to challenge by analyte in which the calibrator response has been used to normalize the test responses. The effect of normalizing to the calibrator values is to reduce the coefficient of variations of $T_1$ and $T_2$ from 27% and 22% to 15% and 14%, respectively.

the standard curve. In the absence of a calibrator, the variation essentially eliminates the possibility of all but semiquantitative measurements. Fig. 8 shows an example of the potential improvement in reproducibility that can be achieved by employing a calibrator. The approach depends on a multianalyte capability. Fig. 8(a) shows a series of individual chip arrays. The horizontal scale describes particular chip arrays. The vertical scale is a measure of the response rate to a challenge of analyte. In Fig. 8(a), the response rate has been normalized to the gating amplitude of each measure. This is equivalent to reporting on the inverse of the time constant of an exponential fit to the response.

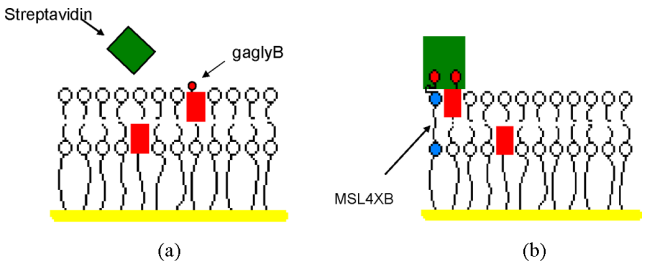


Fig. 9. Illustration of the mechanism responsible for change in performance upon storage (a) Schematic of a sensor membrane containing gaglyB, the short linker biotinylated gramicidin ion channel, and no biotinylated membrane spanning lipid −MSL4XB. (b) Same construct containing +MSL4XB.

In Fig. 8(b), the response rate of each chip is normalized to the gating amplitude of the calibration channel data. This results in a substantial improvement in reproducibility. The provision of a calibrator channel is a significant benefit brought by simultaneous multianalyte detection.

### *B. Stability and Storage*

A key requirement for a diagnostic technology is the ability to store cell-integrated sensors for extended periods with minimal degradation in performance. Fig. 9(a) shows a schematic of a sensor containing the biotinylated gramicidin analog, gaglyB, being gated by the multivalent protein, streptavidin (molecular weight 60 kDa). It was found that if the linker attaching the biotins to the ion channel was reduced in length to a glycine group, then the on-rate for the binding of streptavidin with biotin was ineffective in achieving gating on the 5–10 min timescale. However, as shown in Fig. 9(b), if the membrane spanning lipid, MSL4XB, is present (this has a far longer linker between the biotin and the tethered lipid), a strong rapid gating occurs. The experimental evidence for this is shown in Fig. 10(a) and (b). This suggests that streptavidin binds to the biotin attached by the longer linker on the MSL4XB but not to the biotin attached by a shorter linker on the gaglyB. However, once bound to MSL4XB, the streptavidin is presented in a way to permit gating of the gaglyB. It is proposed that gating of the gaglyB only occurs from the gaglyB diffusing to a site where streptavidin has already bound to the MSL4XB. This provides a method of determining the average diffusion distance of the ion channel in the membrane and a means of probing whether this distance alters on storage. By titrating the gating reaction rate to the concentration of the streptavidin challenge, the on-rate of streptavidin to the MSL4XB, $f_1$, is determined. This may be contrasted with the far slower on-rate of the streptavidin to the gaglyB. Comparing these $f_1$ values with those obtained from directly cross-linking ion channels possessing longer 5XB linkers, it is possible to determine the diffusion distance. The various combinations of $f_1$ are given in Table II. In Table II, it is evident that when using the longer 5XB linkers the dependence on the MSL4XB is almost eliminated.

The ratio of the slopes of Case 2 and Case 3 in Table II provides a measure of the reaction rate, $f_1$. The ratio is 0.17 meaning that the density of mobile channels is greater than the

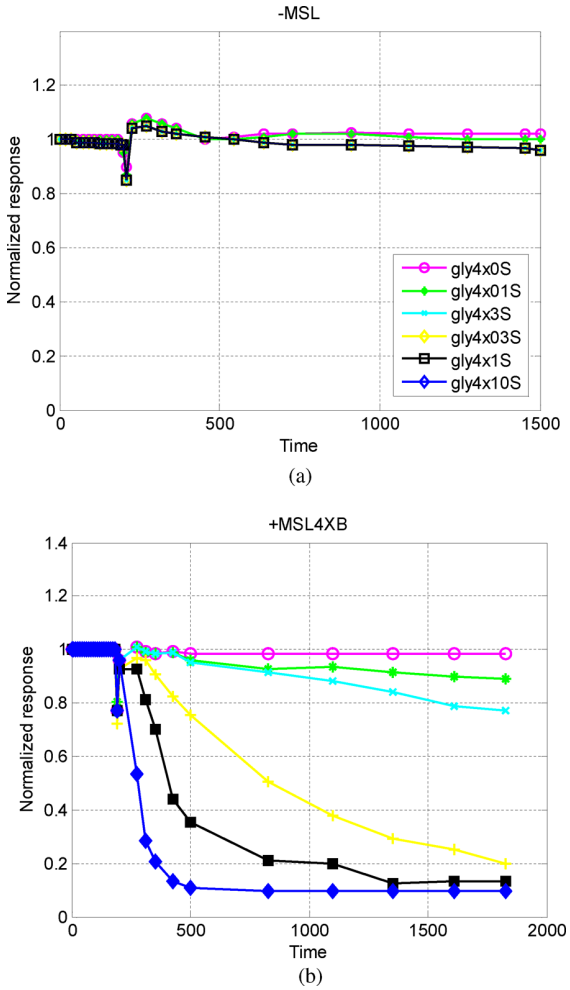


Fig. 10. Experimental gating result for the membrane challenged by 0, 0.1, 0.3, 1, 3, or 10 nM streptavidin. (a) With no MSL4XB, little response is seen at all streptavidin concentrations. (b) With MSL4XB with 0, 0.1, 0.3, 1, 3, or 10 nM streptavidin causes a progressively larger faster response.

TABLE II
EXPERIMENTALLY DETERMINED $f_1$ VALUES FOR THE VARIOUS COMBINATIONS OF ION CHANNEL AND MSL4XB DESCRIBED EARLIER

| Case | Configuration | Slope $= f_1$ ($\mathrm{M}^{-1}\mathrm{s}^{-1}$) |
|---|---|---|
| 1 | gA5XB + MSL4XB | $7.40 \times 10^6$ |
| 2 | gAglyB + MSL4XB | $1.19 \times 10^6$ |
| 3 | gA5XB No MSL4XB | $6.90 \times 10^6$ |
| 4 | gAglyB No MSL4XB | $0.43 \times 10^6$ |

density of the tethered membrane spanning lipid MSL4XB capture sites. This is necessary if streptavidin is used as a species for linking the channel or the tethered lipid to the biotinylated antibodies. However, higher levels of MSL4XB result in substantial cross linking of gA5XB to MSL4XB by the streptavidin. This problem is eliminated by using a covalent linkage to the antibody fragment. Such a covalent linkage allows for larger densities of MSL4XB resulting in significantly higher sensitivities. In the present study, since the density of channels added in the mobile layer is $3 \times 10^9$ molecules/cm$^2$, the MSL4XB density is $6.7 \times 10^8$ molecules/cm$^2$. We refer to this estimate as the *standard density*. Varying the MSL4XB density relative to this standard density permits us to estimate the diffusion distance of the ion channels.

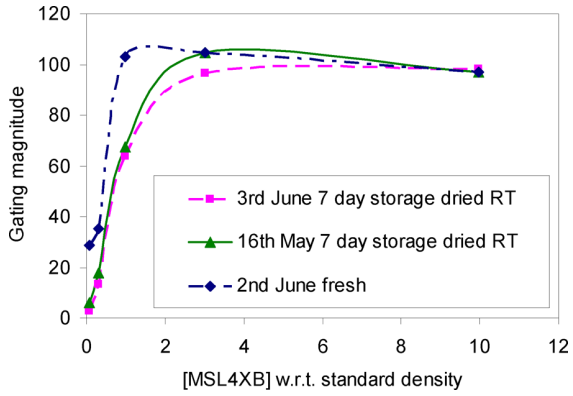


Fig. 11. Plot of gating magnitude versus MSL4XB density relative to the standard density of $6.7 \times 10^8$ molecules/cm$^2$. Drying and storage for two weeks at 20 °C causes a need for higher densities of MSL4XB to achieve the same gating magnitude. Increasing capture site density improves both storage and sensitivity of the sensor.

Fig. 11 illustrates the MSL4XB density plotted relative to the standard density. It can be seen that when the sensors are fresh, the gating amplitude rises from a very low value at zero MSL4XB to a maximal value at approximately the standard density of MSL4XB. This indicates a diffusion distance of the channels of $(6.7 \times 10^8)^{-0.5}$ cm $\approx 0.4\,\mu$m. This further suggests that the membrane surface has a complex structure that restricts the diffusion distance. If the diffusion were unrestricted, a diffusion distance ten times this value would be expected based on reported values of the self-diffusion coefficient of gramicidin in lipid bilayers. When the sensors are dried and stored, the diffusion distance is reduced approximately by 40%. This implies that drying and storage further restricts the average diffusion distance (see Fig. 11). To maintain a gating response for long periods of storage requires increasing the density of MSL4XB.

## VI. CONCLUSION

This paper has provided a detailed description of construction and operation of an ICS biosensor. Fabrication issues such as miniaturization and multiplexing were addressed. A clinical study detailing the use of the ICS biosensor in detecting influenza A virus in untreated clinical samples was discussed. Reproducibility and storage issues were also discussed together with improvements made to the ICS biosensor. This paper sets the stage for the companion paper (Part II), which constructs dynamical models for the ICS biosensor and uses statistical signal processing algorithms to estimate the analyte.

## REFERENCES

[1] B. Hille, *Ionic Channels of Excitable Membranes*, 3 ed. Sunderland, MA: Sinauer Associates, Inc., 2001.

[2] S. H. Chung, O. Anderson, and V. Krishnamurthy, Eds., *Biological Membrane Ion Channels: Dynamics, Structure and Applications*. New York: Springer-Verlag, 2007.

[3] B. Cornell, V. L. Braach-Maksvytis, L. G. King, P. D. Osman, B. Raguse, L. Wieczorek, and R. J. Pace, "A biosensor that uses ion-channel switches," *Nature*, vol. 387, pp. 580–583, 1997.

[4] G. Woodhouse, L. King, L. Wieczorek, P. Osman, and B. Cornell, "The ion channel switch biosensor," *J. Mol. Recognit.*, vol. 12, no. 5, pp. 328–334, 1999.

[5] B. Cornell, G. Krishna, P. Osman, R. Pace, and L. Wieczorek, "Tethered bilayer lipid membranes as a support for membrane-active peptides," *Biochem. Soc. Trans.*, vol. 29, no. 4, pp. 613–617, 2001.

[6] B. Cornell, "Membrane-based biosensors," in *Optical Biosensors: Present and Future*, F. S. Ligler and C. A. R. Taitt, Eds. Amsterdam, The Netherlands: Elsevier, 2002, p. 457.

[7] F. Separovic and B. Cornell, "Gated ion channel-based biosensor device," in *Biological Membrane Ion Channels*, S. H. Chung, O. Andersen, and V. Krishnamurthy, Eds. New York: Springer-Verlag, 2007, pp. 595–621.

[8] E. Neher, "Molecular biology meets microelectronics," *Nature Biotechnol.*, vol. 19, pp. 121–124, Feb. 2001.

[9] D. Georganopoulou, "Reagentless electrochemical biosensors for clinical diagnostics," presented at the 41st Annu. Oak Ridge Conf., Baltimore, MD, Apr. 2009.

[10] M. C. Peterman, J. M. Ziebarth, O. Braha, H. Bayley, H. A. Fishman, and D. M. Bloom, "Ion channels and lipid bilayer membranes under high potentials using microfabricated apertures," *Biomed. Microdevices*, vol. 4, pp. 236–236, 2002.

[11] S. Howorka, J. Nam, H. Bayley, and D. Kahne, "Stochastic detection of monovalent and bivalent protein–ligand interactions," *Angew. Chem. Int. Ed.*, vol. 43, pp. 842–846, 2004.

[12] F. S. Ligler, T. L. Fare, E. E. Seib, J. W. Smuda, A. Singh, P. Ahl, M. E. Ayers, A. W. Dalziel, and P. Yager, "Fabrication of key components of a receptor-based biosensor," *Med. Instrum.*, vol. 22, pp. 247–256, 1988.

[13] R. Naumann, E. K. Schmidt, A. Jonczyk, K. Fendler, B. Kadenbach, T. Liebermann, A. Offenhausser, and W. Knoll, "The peptide tethered lipid membrane as a biomimetic system to incorporate cytochrome c oxidase in a functionally active form," *Biosens. Bioelectron.*, vol. 14, no. 7, pp. 651–662, 1999.

[14] J. Li-Fries, *Ion channels in mixed tethered bilayer lipid membranes*, Ph.D. dissertation, Max Planck Institut für Polymerforschung, Mainz, Germany, 2007.

[15] S. Heysel, H. Vogel, M. Sanger, and H. Sigrist, "Covalent attachment of functionalized lipid bilayers to planar waveguides for measuring protein binding to biomimetic membranes," *Protein Sci.*, vol. 4, no. 12, pp. 2532–2544, 1995.

[16] X. D. Lu, A. L. Ottova, and H. T. Tien, "Biophysical aspects of agar-gel supported bilayer lipid membranes: A new method for forming and studying planar bilayer lipid membranes," *Bioelectrochem. Bioenerg.*, vol. 39, no. 2, pp. 285–289, 1996.

[17] C. A. Naumann, W. Knoll, and C. W. Frank, "Hindered diffusion in polymer-tethered membranes: A monolayer study at the air–water interface," *Biomacromolecules*, vol. 2, no. 4, pp. 1097–1103, 2001.

[18] C. Steinem, A. Janshoff, W. P. Ulrich, M. Sieber, and H. J. Galla, "Impedance analysis of supported lipid bilayer membranes: a scrutiny of different preparation techniques," *Biochim. Biophys. Acta.*, vol. 1279, pp. 169–180, 1996.

[19] E. Sackmann, "Supported membranes: Scientific and practical applications," *Science*, vol. 271, pp. 43–48, 1996.

[20] A. L. Plant, "Supported hybrid bilayer membranes as rugged cell membrane mimics," *Langmuir*, vol. 15, pp. 5128–5135, 1999.

[21] K. Motesharei and M. R. Ghadiri, "Diffusion-limited size-selective ion sensing based on SAM-supported peptide nanotubes," *J. Amer. Chem. Soc.*, vol. 119, pp. 11306–11312, 1997.

[22] J. Bufler, S. Kahlert, S. Tzartos, A. Maelicke, and C. Franke, "Activation and blockade of mouse muscle nicotinic channels by antibodies directed against the binding site of the acetylcholine receptor," *J. Physiol. Lond.*, vol. 492, pp. 107–114, Apr. 1996.

[23] A. N. Lopatin, E. N. Makhina, and C. G. Nichols, "The mechanism of inward rectification of potassium channels: long-pore plugging by cytoplasmic polyamines," *J. Gen. Physiol.*, vol. 106, pp. 923–955, Nov. 1995.

[24] T. Stora, J. H. Lakey, and H. Vogel, "Ion-channel gating in transmembrane receptor proteins: Functional activity in tethered lipid membranes," *Angew. Chem. Int. Ed.*, vol. 38, pp. 389–392, 1999.

[25] Y. Fang, B. Persson, S. Löfås, and W. Knoll, "chapter Chapter 6: Surface Plasmon Fluorescence Spectroscopy for Protein Binding Studies," in *Protein Microarray Technology.*, Wiley–InterScience, 2004, pp. 131–151.

[26] E. Sinner and W. Knoll, "Functional tethered membranes," *Curr. Opin. Chem. Biol.*, vol. 5, no. 6, pp. 705–711, 2001.

[27] L. Scheibler, P. Dumy, H. Boncheva, K. Leufgen, H. J. Mathieu, M. Mutter, and H. Vogel, "Functional molecular thin films: Topological templates for the chemoselective ligation of antigenic peptides to self-assembled monolayers," *Angew. Chem. Int. Ed.*, vol. 38, pp. 696–699, 1999.

[28] G. Woodhouse, L. G. King, and B. A. Cornell, "Kinetics of the competitive response of receptors immobilised to ion-channels which have been incorporated into a tethered bilayer," *Faraday Discuss.*, vol. 111, pp. 247–258, 1999.

[29] R. D. Hotchkiss and R. J. Dubois, "Fractionation of bactericidal agent from cultures of a soil bacillus," *J. Biol. Chem.*, vol. 132, pp. 791–792, 1940.

[30] B. A. Wallace, "Recent advances in the high resolution structures of bacterial channels: Gramicidin A," *J. Struct. Biol.*, vol. 121, no. 2, pp. 123–141, 1998.

[31] S. C. Kushwaha, M. Kates, G. D. Sprott, and I. C. Smith, "Novel complex polar lipids from the methanogenic archaebacterium *Methanospirillum hungatei*," *Science*, vol. 211, pp. 1163–1164, 1981.

[32] M. De Rosa, M. A. Gamacorta, B. Nicolaus, B. Chappeand, and P. Albrecht, "Isoprenoid ethers; backbone of complex lipids of the archaebacterium *Sulfolobus solfataricus*," *Biochim. Biophys. Acta*, vol. 753, pp. 249–256, 1983.

[33] A. Gliozzi, R. Rolandi, M. De Rosa, and A. Gamacorta, "Monolayer black membranes from bipolar lipids of archaebacteria and their temperature-induced structural changes," *J. Membrane Biol.*, vol. 75, no. 1, pp. 45–56, 1983.

[34] R. Naumann, E. K. Schmidt, A. Jonczyk, K. Fendler, B. Kadenbach, T. Liebermann, D. Philip, and J. F. Stoddart, "Self-assembly in natural and unnatural systems," *Angew. Chem. Int. Ed.*, vol. 35, no. 11, pp. 1154–1196, 1996.

[35] T. Kok, L. D. Mickan, and C. J. Burrell, "Routine diagnosis of seven respiratory viruses and *Mycoplasma pneumoniae* by enzyme immunoassay," *J. Virol. Methods*, vol. 50, pp. 87–100, 1994.

[36] B. Stone, J. Burrows, S. Schepetiuk, G. Higgins, A. Hampson, R. Shaw, and T. W. Kok, "Rapid detection and simultaneous subtype differentiation of influenza A viruses by real time PCR," *J. Virol. Methods*, vol. 117, pp. 103–112, 2004.

[37] S. K. Schepetiuk and T. Kok, "The use of MDCK, MEK and LLC-MK2 cell lines with enzyme immunoassay for the isolation of influenza and parainfluenza viruses from clinical specimens," *J. Virol. Methods*, vol. 42, pp. 241–250, 1993.


**Vikram Krishnamurthy** (S'90–M'91–SM'99–F'05) was born in 1966. He received the Bachelor degree from the University of Auckland, Auckland, New Zealand, in 1988, and the Ph.D. degree from the Australian National University, Canberra, A.C.T., Australia, in 1992.

He currently is a Professor and the Canada Research Chair in the Department of Electrical Engineering, University of British Columbia, Vancouver, BC, Canada. Prior to 2002, he was a Chaired Professor in the Department of Electrical and Electronic Engineering, University of Melbourne, Melbourne, Vic., Australia, where he was also the Deputy Head of department. He was an Associate Editor for several journals, including the *Systems and Control Letters*. His current research interests include computational game theory and stochastic control in sensor networks, and stochastic dynamical systems for modeling of biological ion channels and biosensors.

Dr. Krishnamurthy has was an Associate Editor for several journals, including the IEEE TRANSACTIONS AUTOMATIC CONTROL, the IEEE TRANSACTIONS ON SIGNAL PROCESSING, the IEEE TRANSACTIONS AEROSPACE AND ELECTRONIC SYSTEMS, and the IEEE TRANSACTIONS NANOBIOSCIENCE. In 2009 and 2010, he is a Distinguished Lecturer for the IEEE Signal Processing Society. Since 2010, he has been the Editor-in-Chief of the IEEE JOURNAL SELECTED TOPICS IN SIGNAL PROCESSING.

**Sahar Moradi Monfared** received the Bachelor degree in electrical in 2007 from the University of British Columbia, Vancouver, BC, Canada, where she is currently working toward the Masters of Applied Science degree in electrical engineering.

**Bruce Cornell** held a Commonwealth Scientific and Industrial Research Organization (CSIRO) Postdoctoral Fellowship at the University of London (1975–1977) and returned to Australia to a senior scientific post with CSIRO in the field of biophysics. He was appointed the Director of the Cooperative Research Centre for Molecular Engineering (1992–1999) and founded the commercial consortium that became Ambri Ltd., for whom he worked as the Chief Scientist (2000–2005). In 2005, he founded Surgical Diagnostics Ltd., St Leonards, N.S.W., Australia, where he is currently the Director of Science and Technology.

Mr. Cornell is an Elected Member of the Australian Academy of Technological Sciences and Engineering and a member of a number of advisory groups to Australian Universities and an advisory to the Australian Government on the Medical Device Industry.

## QUERIES

Q1: Author: Please supply your own keywords or send a blank e-mail to keywords@ieee.org to receive a list of suggested keywords.

Q2. Author: Please provide the publisher location in Ref. [25].

Q3. Author: Please provide the degree title (B.Sc., M.Sc., Ph.D., etc.), subject (electrical engineering, physics, mathematics, etc.), university names, and the years in which B. Cornell received the degree.